

# Enhancing optical performance of dual-layer remote phosphor structures with the application of $\text{LaAsO}_4:\text{Eu}^{3+}$ and $\text{Y}_2\text{O}_3:\text{Ho}^{3+}$

N. T. P. LOAN, N. D. Q. ANH\*

*Faculty of Electrical and Electronics Engineering, Ton Duc Thang University, Ho Chi Minh City, Vietnam*

Though remote phosphor structure is not an optimal solution for color quality of WLEDs, it is more beneficial to the LED's lumen output than the conformal coating or in-cup phosphor structures. Acknowledging the ability of remote phosphor structure, many researches have been conducted to surmount the disadvantage of this structure in color quality. In this research article, a dual-layer remote phosphor structure with the improvement of color rendering index (CRI) and color quality ratio (CQS) of the WLED is reported. The WLED packages used in this study have the color temperature of 8500 K. The configuration of the phosphor structure will be built by placing a layer of green  $\text{Y}_2\text{O}_3:\text{Ho}^{3+}$  or red  $\text{LaAsO}_4:\text{Eu}^{3+}$  phosphor on the yellow  $\text{YAG}:\text{Ce}^{3+}$  phosphor layer. Then, the concentration of added phosphor  $\text{LaAsO}_4:\text{Eu}^{3+}$  will be adjusted to get the highest chromatic homogeneity. The experimental results demonstrated the rise in CRI and CQS values with the added  $\text{LaAsO}_4:\text{Eu}^{3+}$ , which means the presence of  $\text{LaAsO}_4:\text{Eu}^{3+}$  has a great effect on these two aspects. Specifically, due to the growth of red light components inside WLEDs packages, the more the concentration of  $\text{LaAsO}_4:\text{Eu}^{3+}$  is added, the better the CRI and CQS become. Meanwhile, with green phosphor  $\text{Y}_2\text{O}_3:\text{Ho}^{3+}$ , the luminous flux is benefited. Nevertheless, when the concentrations of both red  $\text{LaAsO}_4:\text{Eu}^{3+}$  and green  $\text{Y}_2\text{O}_3:\text{Ho}^{3+}$  phosphors surpass the corresponding level, the luminescent efficiency and color quality are reduced. This result is demonstrated based on the Mie-scattering theory and Lambert-Beer's law. The findings in this research are important references for manufacturing WLED packages with improved white-light quality.

(Received December 16, 2019; accepted February 12, 2021)

**Keywords:** WLEDs, Mie-scattering theory, Color rendering index, WLEDs,  $\text{Y}_2\text{O}_3:\text{Ho}^{3+}$ ,  $\text{LaAsO}_4:\text{Eu}^{3+}$ , Lumen output, Color quality, Mie-scattering theory

## 1. Introduction

As illumination market has higher demands in lighting solution these days, the solid-state lighting (SSL) has been recognized for its advantages that are much better than the other lighting solutions. One of the most used sources of illumination for (SSL) is phosphor converted white light emitting diodes (pc-WLEDs) as it is simpler to fabricate than the other ones [1]. The popularity of white light-emitting diodes in our daily life is undeniable. They are utilized in many aspects, often in transportation lighting (vehicle lights, traffic lights, street lights...), residential lighting, entertainment or commercial lighting (backlighting...), and more. However, there are two principal factors that white LEDs need improvements to widespread their usage: the light extraction efficiency and the angular homogeneity of correlated color temperature [2]. Thus, further breakthroughs in lumen output and color quality of WLEDs are essentials to fulfill high demands of the market as well as requirements of life applications [3]. One of the most common methods to improve this potential light source is the one based on the combination of yellow lights collected from the converse red phosphor with blue lights generated from the blue LED chip. It is undeniable that the factors have determining effects on the

efficiency of lumen output and mostly on the color rendering index (CRI) are the LEDs' structure and the arrangement of phosphor layers [4-8]. Therefore, there are many phosphor coating techniques that have been commonly applied to pc-WLEDs' production, including dispensing and conformal phosphor coating methods [9, 10]. However, the color quality of these structures is low since the phosphors cannot convert light effectively due to the damage cause by the heat from the light source. In particular, when the phosphor layer is directly placed on the LED chip surface, the heat released from the chip straightly reaches and impacts the phosphors, then degrading the lighting conversion of the material. Hence, to enhance the performance of phosphor layers and avoid the irreversible destruction to the phosphor, a reduction in the thermal outcome is essential. In several previous researches, it is showed that the remote phosphor structure can reduce the heat effect as the phosphor layers of this structure are placed distantly from the LED chip which is also known as a heat source. It is an appropriate distance between the phosphor layers and the LED chip that could allow the LEDs to limit the backscattered and circulated lights inside the package. So, remote phosphor configuration turned out to be the best solution for LED-chip heat control, and the lumen efficacy and color quality

of LEDs can be improved significantly [11-16]. The WLED remote phosphorus model can manage to comply with the requirements of lighting devices for simple daily activities but for those of other advanced illumination applications, it cannot completely fulfil. Thus, the development of the next WLED's generation is understandable and essential. For the next upgrade LEDs packages, significant developments were made for remote phosphor structures to reduce the backscattering events in the phosphor layer, from which the enhancement in luminous efficiency can be achieved. A study demonstrated that the configuration of a remote phosphor layer surrounding an inverted cone lens encapsulant could acquire the considerable reduction in the amount of reflected light loss, since it can adjust the direction of light from the LED straight to the LED surface [17]. Besides, using a sapphire-patterned remote phosphor configuration without coating phosphor on the perimeter area could accomplish high angular correlated color temperature (CCT) homogeneity and color consistency [18]. Moreover, the patterned sapphire substrate is more beneficial to the remote phosphorus structure as this pattern could manage to accomplish the uniform in chromatic distribution in a far field pattern than a conventional pattern [19]. Thus, the dual-layer remote phosphor structure is proposed to accomplish the enhancement in the light output of LED's packages. Previous studies have focused on the improvement of the consistent chromaticity and the lumen output of WLEDs when using the remote phosphor structure; however, the WLEDs in these studies used single chip structure and having low color temperatures. Meanwhile, enhancing the optical parameters for pc-WLED devices having high color temperature is a difficult and complicated task. In addition, the comparison of the effectiveness among different dual-layer phosphorus configurations has not been demonstrated in any previous study. Thus, it is hard for manufacturers to determine an optimal remote phosphor layer structure to optimize the angular CCT quality and lumen efficacy of WLEDs.

To achieve the goal of enhancing the color quality of WLEDs at high color temperature 8500 K, this research paper introduces two distinguished dual-layer remote phosphor structures. One remote phosphor model uses green phosphor layer  $Y_2O_3:Ho^{3+}$  for increasing the green light component in WLEDs, leading to the higher luminous flux; meanwhile, the other adds the red  $LaAsO_4:Eu^{3+}$  phosphorus layer to get a growth in the red light component to better the CRI and CQS values. Moreover, this study gives a detailed description of the chemical composition of  $LaAsO_4:Eu^{3+}$  that contributes significantly to the change in optical performances of WLEDs. Besides, the findings from this research showed that there is a noticeable improvement in the values of CRI and CQS when the phosphor  $LaAsO_4:Eu^{3+}$  is added. However, when the blue or red phosphor concentrations rise excessively, it is essential to modify the concentrations of  $Y_2O_3:Ho^{3+}$  and  $LaAsO_4:Eu^{3+}$  to an appropriate amount to prevent a steep decline in chromatic consistency or luminescence. From the results of the studies, there are three main differences when having a

green or red phosphor layer along with the existing  $YAG:Ce^{3+}$  yellow phosphorus. First, the greater amount of supplemented blue or red light components can increase the spectrum of white light. This is the main point in improving LED-light angular CCT homogeneity. Second, the light scattering and transmission in the phosphor configuration are opposite to the concentration of the added phosphor layers. That's why, determining an appropriate amount for phosphor concentrations is an important task to get the luminous flux of WLEDs enhanced.

## 2. Detail of experiment and simulation

### 2.1. Preparation of phosphor materials

Before constructing the remote phosphor configurations, red and green phosphors,  $LaAsO_4:Eu^{3+}$  and  $Y_2O_3:Ho^{3+}$ , must be prepared with the ingredients having mole percent and weight listed in the Table 1 and Table 2 [20].

Table 1. Ingredients of  $LaAsO_4:Eu^{3+}$  phosphor composition

| Ingredient | Mole (%)    | By weight (g) |
|------------|-------------|---------------|
| $La_2O_3$  | 95 (of La)  | 155           |
| $Eu_2O_3$  | 5 (of Eu)   | 8.8           |
| $As_2O_3$  | 100 (of As) | 75            |

The preparation process of  $LaAsO_4:Eu^{3+}$  composition includes two stages of firing. However, before being fired, the materials have to go through some initial steps. First, the ingredients are mixed together by slurring in 30%  $H_2O_2$ . Then, the mixture is heated up gently and stirred until its boiling indicates formations of  $H_3AsO_4$ . After that, it will be dried in air and powderized. After this step, the first firing stage will be started. The powderized material will be fired in open quartz boats with air and at the temperature of approximate  $500^{\circ}C$ . When this process is finished, the product will be taken out and powderized for the second time. Next, it is put into open quartz boats for the second firing process. This time, the firing will be carried out with air, at  $1000^{\circ}C$  and last for 1 hour. Finally, when 1 hour of firing is over, we will get the red phosphor  $LaAsO_4:Eu^{3+}$  with emission peak from 1.785 to 2.149 eV.

Table 2. Ingredients of  $Y_2O_3:Ho^{3+}$  composition

| Ingredient | Mole %      | By weight (g) |
|------------|-------------|---------------|
| $Y_2O_3$   | 100 (of Y)  | 108           |
| $Bi_2O_3$  | 0.1 (of Bi) | 0.230         |
| $CaF_2$    | 2.5         | 1.95          |

Similar to the preparation of  $LaAsO_4:Eu^{3+}$ , that of  $Y_2O_3:Ho^{3+}$  consists of two firing processes, but first, the

ingredients must be mixed by slurring in water or methanol. Then, drying the mixture in air, and after that powderizing it. Next, the first firing of the material will be carried out in capped quartz tubes with stagnant air for an hour at  $1300^\circ\text{C}$ . When the firing time is over, the product will be powderized. Then, it will be fired for the second time in capped quartz tubes with the same condition as the first firing process. The obtained  $\text{Y}_2\text{O}_3:\text{Ho}^{3+}$  will have emission peak with two visible lines at 2.266 and 2.30 eV in addition to many lines in the IR.

## 2.2. Simulation process

In our experiments, we precisely built WLED models based on actual WLED packages having high performance in optical-thermal stability, as detailed in Table 3. The normalized cross correlations between the simulated and the actual models are approximately 99.6%. Besides, there may have some reductions in the CRI and CCT of WLED due to the effects of LED features, including wavelength, waveform, light intensity, and operating temperature. For the phosphor-compounding simulation, we utilized the LightTools program. It is noted that the phosphor weight is controlled during simulation process carried out with this program.

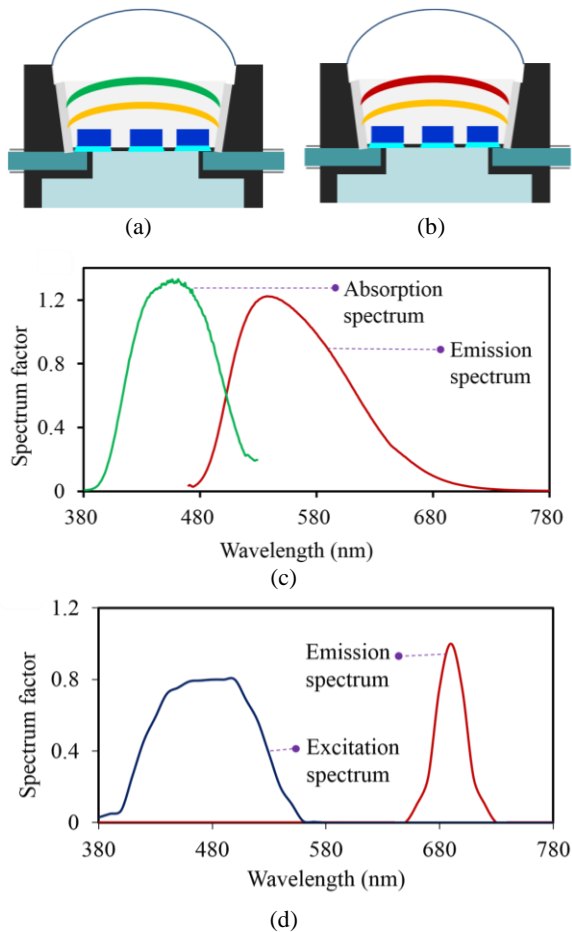
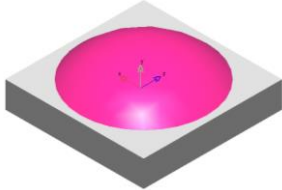
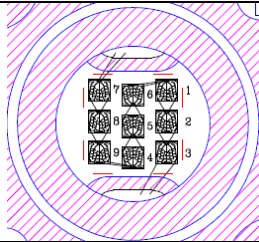


Fig. 1. (a) Illustration of GYC, (b) RYC, (c) the measured spectra of the yellow-emitting  $\text{YAG}:\text{Ce}^{3+}$  phosphor, (d) the measured spectra of the red-emitting  $\text{LaAsO}_4:\text{Eu}^{3+}$  phosphor (color online)

This article proposed two dual-layer remote phosphor configurations of the green-yellow phosphor (GYC) and red-yellow phosphor (RYC). Both structures, GYC and RYC, are constructed with two phosphor films placed above and separated from the nine blue chips. Specifically, in GYC structure, the layer of phosphor  $\text{Y}_2\text{O}_3:\text{Ho}^{3+}$  is above  $\text{YAG}:\text{Ce}^{3+}$  yellow phosphor layer, see Fig. 1 (a). Meanwhile, in RYC structure the phosphor layer of  $\text{LaAsO}_4:\text{Eu}^{3+}$  is set above  $\text{YAG}:\text{Ce}^{3+}$  yellow phosphor layer, as illustrated in Fig. 1 (b). The purpose of applying these two remote phosphorus configurations is to get the improvement in the color uniformity and lumen efficacy for the pc-WLEDs. This goal can be reached by pushing the green scattering and red light component inside the WLED's packages. Nevertheless, to succeed in doing this, the concentrations of  $\text{Y}_2\text{O}_3:\text{Ho}^{3+}$  and  $\text{LaAsO}_4:\text{Eu}^{3+}$  phosphors must be adjusted accordingly. In addition, Fig. 1(c) presents the measured absorption spectrum and emission spectrum of yellow-emitting phosphor  $\text{YAG}:\text{Ce}^{3+}$ , and Fig. 1 (d) demonstrates the  $\text{LaAsO}_4:\text{Eu}^{3+}$  red phosphor's excitation and emission spectra. Besides, as mentioned in Table 3, each blue chip of the experimented LED model has the lumen power of 1.16 W with the light-emitting wavelength of 453 nm.

Table 3. The actual parameters of LED chip (color online)

|                      |   |
|----------------------|---|
| LED vender           | <i>Epistar</i>  |
| LED chip             | <i>V45H</i>   |
| Voltage (V)          | <i>3.5~3.6</i>  |
| Peak Wavelength (nm) | <i>453</i>  |
| Power (mW)           | <i>320~340</i>  |
| Lead frame           | <i>4.7mm Jentech Size-S</i>   |
| Die attach           | <i>Sumitomo 1295SA</i>  |
| Actual sample        |  |
| Simulated sample     |  |
| Bonding diagram      |  |

As can be seen from Fig. 2, the concentrations green  $\text{Y}_2\text{O}_3:\text{Ho}^{3+}$  and red  $\text{LaAsO}_4:\text{Eu}^{3+}$  phosphors change in the opposite trend to the  $\text{YAG}:\text{Ce}^{3+}$  concentration. This different change will have the average CCTs maintained and influence the light scattering and absorption abilities in the phosphor films of the LED packages. Obviously, this will perform a noticeable impact on not only the color property but also the luminous flux of the LED's lamps. Therefore, the choice of the concentration of these phosphors  $\text{Y}_2\text{O}_3:\text{Ho}^{3+}$  and  $\text{LaAsO}_4:\text{Eu}^{3+}$  is a decisive element for the enhancement of the WLED's color quality. Specifically, as the concentrations of  $\text{Y}_2\text{O}_3:\text{Ho}^{3+}$  and  $\text{LaAsO}_4:\text{Eu}^{3+}$  increase from 2% to 20% wt., the  $\text{YAG}:\text{Ce}^{3+}$  concentration decreases to maintain the average CCT, even the WLEDs have a high color temperature of 8500 K.

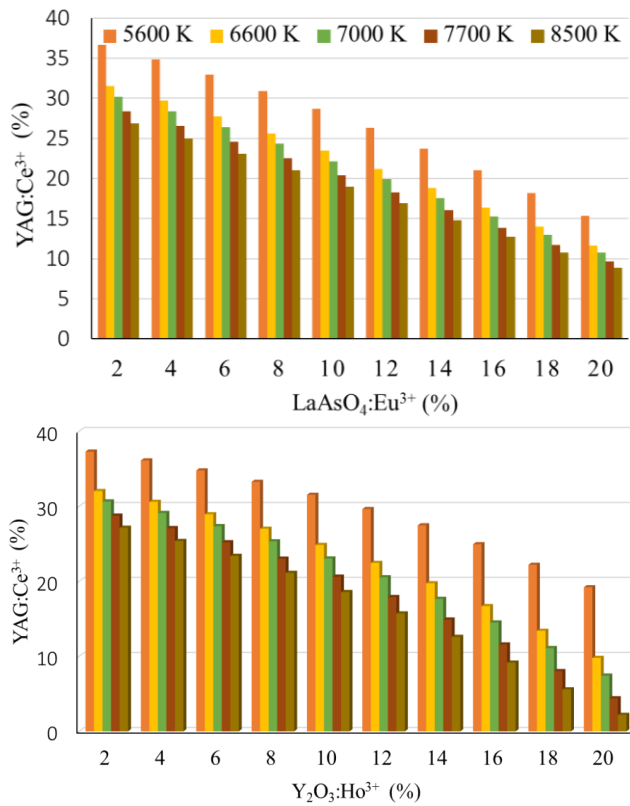


Fig. 2. The change of phosphor concentration of RYC (above) and GYC (below) for keeping the average CCT (color online)

On top of that, as presented in Fig. 3, the effect on the spectrum of WLEDs caused by the concentrations of red  $\text{LaAsO}_4:\text{Eu}^{3+}$  is noticeable. Compared to the structure with green phosphor  $\text{Y}_2\text{O}_3:\text{Ho}^{3+}$ , the red-yellow configuration shows the increase in spectral emission in three different regions. In Fig. 3 (b), the intensity in the spectral regions of 420 nm - 480 nm and 500 nm - 640 nm rise when the  $\text{Y}_2\text{O}_3:\text{Ho}^{3+}$  concentration increases. In other words, the increase of the emission spectra in these two regions shows the better luminous flux. Moreover, with  $\text{Y}_2\text{O}_3:\text{Ho}^{3+}$ , there are more internal scattering events of blue lights, indicating that the phosphor scattering increases inside the LEDs, and as a result, the copper color is benefited. Meanwhile, with the growth of  $\text{LaAsO}_4:\text{Eu}^{3+}$

concentration, the emission spectrum in 648 nm - 738 nm wavelength range shows its increase. Besides, the red phosphor  $\text{LaAsO}_4:\text{Eu}^{3+}$  increases the emission spectra in two wavelength bands similar to the case of the green phosphor  $\text{Y}_2\text{O}_3:\text{Ho}^{3+}$ . This means that the red phosphor is also suitable for increasing the blue light scattering or luminous flux of WLEDs.

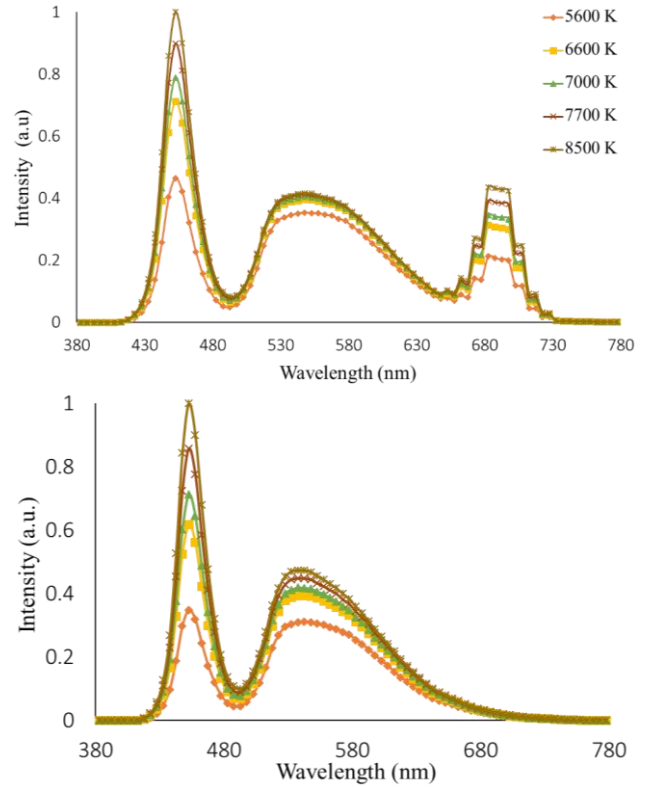


Fig. 3. Emission spectra of RYC (above) and GYC (below) (color online)

One more result that can be observed from Fig. 3 is the rise of emission spectra along with the increase of color temperature. In other words, higher color temperatures result in better emission spectra. Hence, it is possible to achieve better the color and optical quality. This result is an important reference for LEDs production with the application of  $\text{LaAsO}_4:\text{Eu}^{3+}$  phosphor, especially when it is hard to control the quality of WLEDs with high temperature. In brief, the research identifies that red phosphor  $\text{LaAsO}_4:\text{Eu}^{3+}$  can enhance the consistent color performance of WLEDs with high color temperature (8500 K). Based on the requirements of manufacturers, the selection of the structure can be made. If they want to produce the WLEDs with high color quality, it is acceptable to have a small amount of reduced lumen output.

### 3. Computation and discussion

As reported in optical studies, color rendering index (CRI) is a common measurement used in WLED-color-

quality evaluation. Particularly, it evaluates how the light source reveal the true color of the objects in comparison to the natural one. Based on the color principle of the three key colors: red, yellow and green, when the green light component is more than the others, the color imbalance occurs. As a result, the color quality of WLEDs is affected and then, reducing their color integrity. Hence, it seems that the higher concentration of green phosphor  $\text{Y}_2\text{O}_3:\text{Ho}^{3+}$  would damage the chromatic quality of the WLED packages. Fig. 4 demonstrated the CRI of WLED packages with the concentration of  $\text{Y}_2\text{O}_3:\text{Ho}^{3+}$  and  $\text{LaAsO}_4:\text{Eu}^{3+}$  increased from 2% wt. to 20% wt.

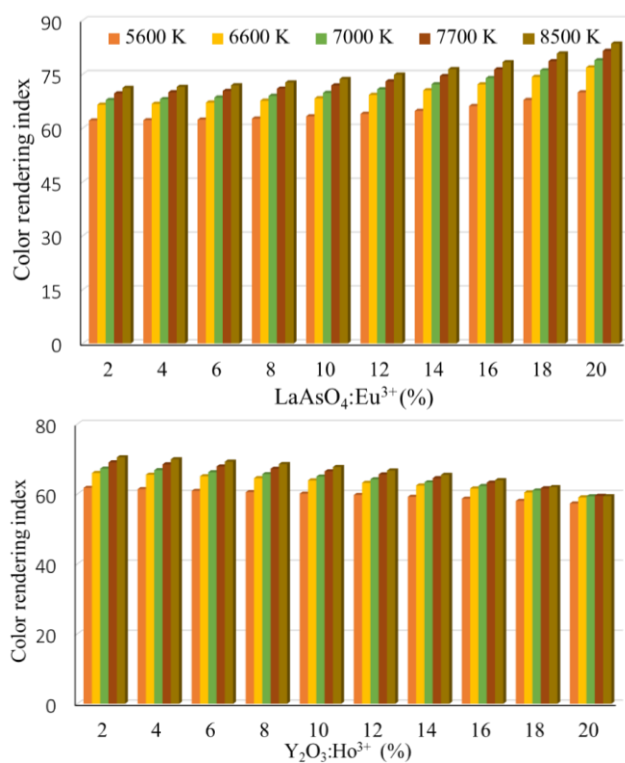


Fig. 4. The color rendering index as a function of the concentration of  $\text{LaAsO}_4:\text{Eu}^{3+}$  (above)  $\text{Y}_2\text{O}_3:\text{Ho}^{3+}$  (below) (color online)

As can be seen, the rise in  $\text{Y}_2\text{O}_3:\text{Ho}^{3+}$  and  $\text{LaAsO}_4:\text{Eu}^{3+}$  concentrations leads to the opposite change between their CRIs. In particular, when  $\text{LaAsO}_4:\text{Eu}^{3+}$  increases, the red light component also rises, enhancing the CRI. In the case of WLED with high CCT of 8500 K, the color rendering index can be promoted from 68 to 82. For the other WLEDs with lower CCTs, their CRI can increase by 20% with higher content of  $\text{LaAsO}_4:\text{Eu}^{3+}$ . The force behind this upward trend of CRI when using red phosphor  $\text{LaAsO}_4:\text{Eu}^{3+}$  in the remote phosphor structure is its absorption feature. This red phosphor can absorb not only the LED-chip excited blue lights but also the phosphor-emitted yellow lights. Moreover, when absorbing the blue light,  $\text{LaAsO}_4:\text{Eu}^{3+}$  will turn blue light into red light. Thus, due to its absorption characteristic, the blue light absorption is stronger than the yellow one

although this red phosphor absorbs two kinds of light. In contrast, the increase of  $\text{Y}_2\text{O}_3:\text{Ho}^{3+}$  from 0 – 20% wt. reduces the CRI by approximately 16%, as can be seen in Fig. 4 (b). This decrease is attributed to the excessively enhanced green-light components when there is higher concentration of  $\text{Y}_2\text{O}_3:\text{Ho}^{3+}$  in the WLED phosphor structure. Meanwhile, the mechanism for improving CRI is to increase red lights with an appropriate proportion, so the enhancement of green light proportion is not beneficial to CRI values [23, 24]. Therefore, the addition of  $\text{LaAsO}_4:\text{Eu}^{3+}$  has the red light component increased, resulting in higher color rendering index (CRI). CRI is a crucial parameter for an efficient modern WLED lamp, so if a LED package has a high color rendering index, its price will be higher than the others. However, when using the  $\text{LaAsO}_4:\text{Eu}^{3+}$ , it is possible to reduce the production cost and lower the price of WLED in the market, which leads to the popularity of its use in LED fabrication. Nevertheless, as mentioned above, researchers have focused on CQS, a more synthetic index to evaluate the color quality of LEDs than CRI [25].

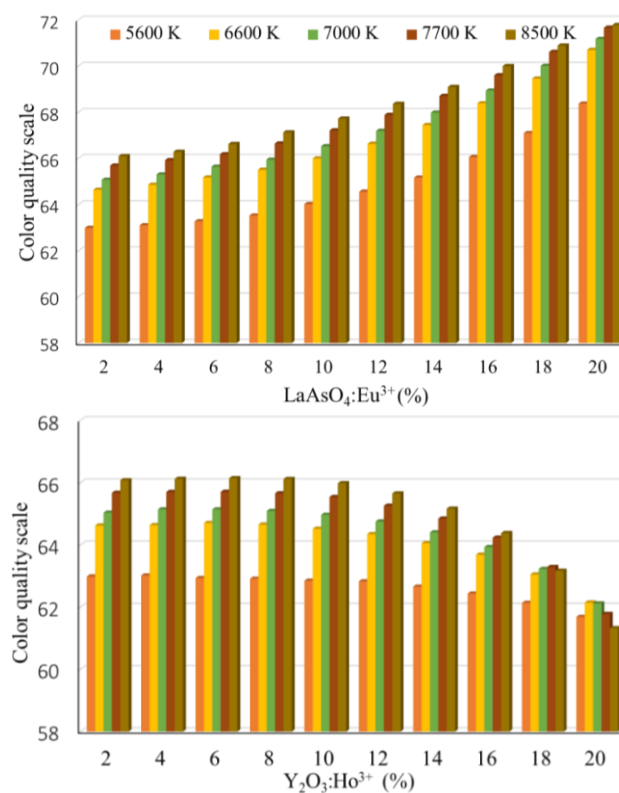


Fig. 5. The color quality scale as a function of the concentration of  $\text{LaAsO}_4:\text{Eu}^{3+}$  (above)  $\text{Y}_2\text{O}_3:\text{Ho}^{3+}$  (below) (color online)

CQS, a parameter for color evaluation, includes three important elements of CRI, viewers' preference and chromaticity coordinates [26, 27]. Fig. 5 showed the contrast of CQS resulted from growing  $\text{Y}_2\text{O}_3:\text{Ho}^{3+}$  and  $\text{LaAsO}_4:\text{Eu}^{3+}$  concentrations to 20% wt. As there is higher  $\text{LaAsO}_4:\text{Eu}^{3+}$  concentration, getting the red-light component boosted, CQS performs higher values;

moreover, the CQS of WLED with 8500 K CCT can be heightened from 66 to 71. Similarly, the WLEDs with lower CCTs can attain approximately 7.6% improvement of CQS. However, the CQS presents significant degradation, about 8.2%, as the concentration of  $Y_2O_3:Ho^{3+}$  develops to 20% wt. The enhanced greenlight components surpassing a certain level is the main cause for this decrease in CQS. Similar to CRI, the enhancement in red light component is the way to better the CQS; thus, green light components do not benefit the CQS [28]. Nevertheless, according to the results from Fig. 5, when the concentration of  $Y_2O_3:Ho^{3+}$  does not exceed 8%, CQS maintains its high values. Therefore, an appropriately selected concentration of  $Y_2O_3:Ho^{3+}$  can fluctuate from 2% to 8% if the goal is to get better color quality, after considering emitted luminous flux. Fig. 5 demonstrated that red phosphor  $LaAsO_4:Eu^{3+}$  can enhance CQS values as it did with the CRI. The first chart in Fig. 5 presented that the significant increase of CQS follows the rise of  $LaAsO_4:Eu^{3+}$  concentration. Therefore, it can be concluded that applying  $LaAsO_4:Eu^{3+}$  phosphor layer can better the quality of white light color for WLEDs constructed with dual-layer remote phosphorus configuration. For the manufacturers aiming at acquiring the advances in color quality of WLEDs, this is one of the most valuable findings to take into account. However, the fact that  $LaAsO_4:Eu^{3+}$  is somehow disadvantage to the lumen output of WLEDs should not be ignored. The scientific model, including the mathematic expressions for calculating the transmitted blue light and converted yellow light of dual-layer remote phosphor configurations, will be presented and proved in this part. Moreover, from this model, it is possible to obtain a tremendous development in WLED efficacy.

In terms of single-layer remote phosphor configuration, its transmitted blue lights and converted yellow lights are expressed as follows. It is noted that the phosphor layer has a thickness of  $2h$  [22], [29].

$$PB_1 = PB_0 \times e^{-2\alpha_{B1}h} \quad (1)$$

$$PY_1 = \frac{1}{2} \frac{\beta_1 \times PB_0}{\alpha_{B1} - \alpha_{Y1}} (e^{-2\alpha_{Y1}h} - e^{-2\alpha_{B1}h}) \quad (2)$$

For the structure of dual-layer remote phosphor having  $h$  thickness for each layer, the calculations of transmitted blue light and converted yellow light are:

$$PB_2 = PB_0 \times e^{-2\alpha_{B2}h} \quad (3)$$

$$PY_2 = \frac{1}{2} \frac{\beta_2 \times PB_0}{\alpha_{B2} - \alpha_{Y2}} (e^{-2\alpha_{Y2}h} - e^{-2\alpha_{B2}h}) \quad (4)$$

In which  $h$  indicates the thickness of each phosphor layer. The subscript "1" is for single-layer phosphorus structure, and "2" is for the dual-layer remote phosphor.  $\beta$  is the conversion coefficient for blue light that converts to yellow light, while  $\gamma$  presents the yellow-light reflection

coefficient. The blue-light intensity ( $PB$ ) and yellow-light intensity ( $PY$ ) express the light intensity from the blue LED, presented by  $PB_0$ . Besides,  $\alpha_B$  and  $\alpha_Y$  characterize the energy-loss fractions of blue and yellow lights, respectively, during their multiplication in the phosphorus layer separately. With the dual-layer remote phosphor configuration, the lighting efficiency of pc-LEDs is much better than the result attained from the single-layer structure:

$$\frac{(PB_2 + PY_2) - (PB_1 + PY_1)}{PB_1 + PY_1} > 0 \quad (5)$$

Based on the Mie-theory [21], the scattering of the phosphor particles was determined, and the scattering cross section  $C_{sca}$  of spherical phosphor grains can be calculated. In addition, the calculation of transmitted light power is performed via the application of the Beer's law [22]:

$$I = I_0 \exp(-\mu_{ext}L) \quad (6)$$

$I_0$  presents the incident light power.  $L$  expresses the phosphor layer thickness (mm).  $\mu_{ext}$  indicates the extinction coefficient. Besides,  $\mu_{ext}$  is computed by:  $\mu_{ext} = N_r C_{ext}$ , in which  $N_r$  ( $mm^{-3}$ ) and  $C_{ext}$  ( $mm^2$ ) are defined as the number density distribution and the extinction cross-section of phosphor particles, respectively.

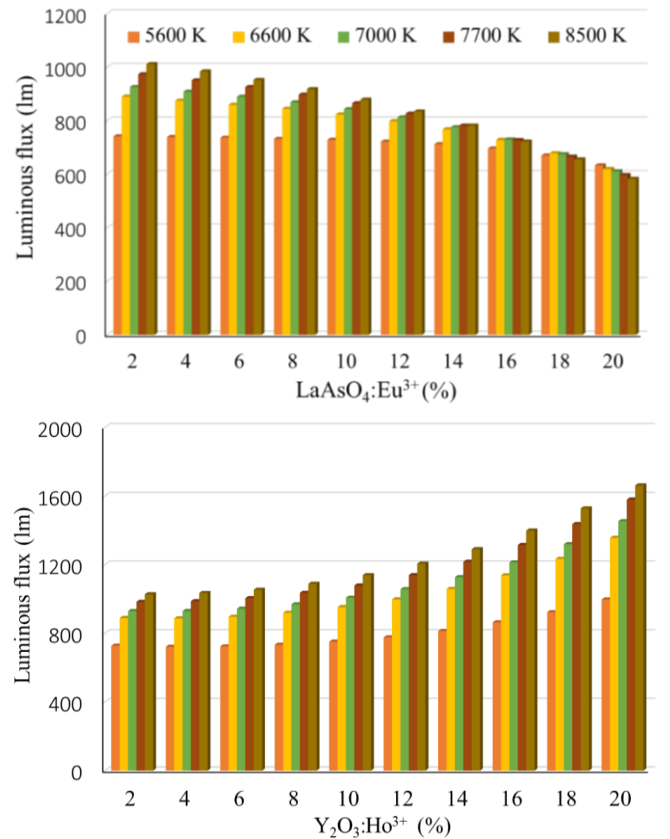


Fig. 6. The lumen output as a function of the concentration of  $LaAsO_4:Eu^{3+}$  (above)  $Y_2O_3:Ho^{3+}$  (below) (color online)

Expression (5) showed that the luminous efficiency of double-layer phosphor configuration of pc-LEDs is better than that of the LED using one-layered phosphor structure. Thus, this research has performed and proved the lumen efficacy of the dual-layer remote phosphor layer applied in LED's packages. In Fig. 6, we can observe the growth of luminous flux when  $\text{Y}_2\text{O}_3:\text{Ho}^{3+}$  is raised from 2% wt. to 20% wt. In contrast, with the increase of  $\text{LaAsO}_4:\text{Eu}^{3+}$  phosphor concentration, the luminous flux of the dual-layer structure shows a sharp decline. Obviously, in line with Lambert-Beer law, the reduction factor  $\mu_{ext}$  is in direct proportion to  $\text{LaAsO}_4:\text{Eu}^{3+}$  layer's concentration while in inverse proportion to the transmission energy of lights. Therefore, if the thicknesses of two phosphor films are fixed, the emitted photoluminescence could decline when the concentration of  $\text{LaAsO}_4:\text{Eu}^{3+}$  rises. However, the luminous flux resulted from the dual-layer configuration (comprising a red  $\text{LaAsO}_4:\text{Eu}^{3+}$  phosphor layer) is better than from the single-layer structure (not using the red phosphor). What's more, this red phosphor also benefits the CRI and CQS values. Therefore, with these advantages achieving from using  $\text{LaAsO}_4:\text{Eu}^{3+}$ , this decrease in lumen output completely acceptable. Manufacturers can choose an appropriate concentration of  $\text{LaAsO}_4:\text{Eu}^{3+}$  to apply for WLEDs mass production, depending on the goal they want to accomplish.

#### 4. Conclusions

In this study, the influences of the green  $\text{Y}_2\text{O}_3:\text{Ho}^{3+}$  and red  $\text{LaAsO}_4:\text{Eu}^{3+}$  phosphors on two color parameters, CRI and CQS, and the luminous performance of dual-layer phosphor structure are demonstrated. Through the application of Mie-scattering theory and the Lambert-Beer law, it can be concluded from the research that  $\text{LaAsO}_4:\text{Eu}^{3+}$  is a suitable phosphor material for the enhancement of color quality, while  $\text{Y}_2\text{O}_3:\text{Ho}^{3+}$  is a right choice for the better luminous flux of WLEDs. With these phosphors applied in dual-layer remote phosphor structure, this result can be attained from the WLED with low or high (8500 K) color temperatures. Thus, this study has accomplished the purpose of promoting the color consistency for WLED lamps, one of the most struggling problems that remote-phosphor structure has to address. However, a small drawback in terms of luminous flux still exists: when the concentrations of  $\text{Y}_2\text{O}_3:\text{Ho}^{3+}$  or  $\text{LaAsO}_4:\text{Eu}^{3+}$  increase over a certain number, the chromatic homogeneity or lumen efficiency tend to decrease. Thus, determining an appropriate concentration of those phosphor is vital for producers to fulfill their goals. Moreover, the results attained from the research paper can be used as crucial references in producing higher-quality WLED packages.

#### References

- [1] G. Z. Zhang, K. Ding, G. X. He, P. Zhong, *OSA Continuum* **2**, 1056 (2019).
- [2] P. Q. Jiang, Y. Peng, Y. Mou, H. Cheng, M. X. Chen, S. Liu, *Appl. Opt.* **56**, 7921 (2017).
- [3] C. W. Zhang, L. C. Xiao, P. Zhong, G. X. He, *Appl. Opt.* **57**, 4665 (2018).
- [4] X. M. Wang, H. B. Rao, W. Zhang, Q. L. Lei, D. Zhou, Q. Zhang, C. N. Li, C. Y. Zhou, *J. Display Technol.* **12**, 1609 (2016).
- [5] B. J. Shih, S. C. Chiou, Y. H. Hsieh, C. C. Sun, T. H. Yang, S. Y. Chen, T. Y. Chung, *Opt. Express* **23**, 33861 (2015).
- [6] X. T. Xiao, H. D. Tang, T. Q. Zhang, W. L. Chen, D. Wu, R. Wang, K. Wang, *Opt. Express* **24**, 21577 (2016).
- [7] W. J. Gao, K. Ding, G. X. He, P. Zhong, *Appl. Opt.* **57**, 9322 (2018).
- [8] C. H. Chiang, T. H. Liu, H. Y. Lin, H. Y. Kuo, S. Y. Chu, *J. Display Technol.* **11**, 466 (2015).
- [9] H. S. Lee, S. H. Kim, J. Heo, W. J. Chung, *Opt. Lett.* **43**, 627 (2018).
- [10] Y. Peng, X. Guo, R. X. Li, H. Cheng, M. X. Chen, *Appl. Opt.* **56**, 3270 (2017).
- [11] W. L. Zhang, W. Yang, P. Zhong, S. L. Mei, G. L. Zhang, G. L. Chen, G. X. He, R. Q. Guo, *Opt. Mater. Express* **7**, 3065 (2017).
- [12] L. C. Xiao, C. W. Zhang, P. Zhong, G. X. He, *Appl. Opt.* **57**, 931 (2018).
- [13] Y. Peng, Y. Mou, X. Guo, X. J. Xu, H. Li, *Opt. Mater. Express* **8**, 605 (2018).
- [14] M. S. Xu, H. X. Zhang, Q. B. Zhou, H. Wang, *Appl. Opt.* **55**, 4456 (2016).
- [15] L. L. Zan, D. Y. Lin, P. Zhong, G. X. He, *Opt. Express* **24**, 7643 (2016).
- [16] A. Q. Zhang, B. Wang, Q. Yan, Y. C. Wang, J. Jia, H. S. Jia, B. S. Xu, W. Y. Wong, *Opt. Mater. Express* **8**, 3635 (2018).
- [17] H. Y. Lin, K. Ju Chen, S. W. Wang, C. C. Lin, K. Y. Wang, J. R. Li, P. T. Lee, M. H. Shih, X. L. Li, H. M. Chen, H. C. Kuo, *Opt. Express* **23**, A27 (2015).
- [18] H. F. Sijbom, R. Verstraete, J. J. Joos, D. Poelman, P. F. Smet, *Opt. Mater. Express* **7**, 3332 (2017).
- [19] H. W. Chen, Z. Y. Luo, R. D. Zhu, Q. Hong, S. T. Wu, *Opt. Express* **23**, 13060 (2015).
- [20] W. M. Yen and M. J. Weber, *Inorganic Phosphors: Compositions, Preparation and Optical Properties*, (CRC Press, LLC, 2000 N.W. Corporate Blvd., Boca Raton, Florida 33431, 2004).
- [21] F. Li, L. You, C. Nie, Q. Zhang, X. Jin, H. Y. Li, X. B. Gu, Y. Huang, Q. H. Li, *Opt. Express* **25**, 21901 (2017).
- [22] N. D. Q. Anh, P. X. Le, H. Y. Lee, *Curr. Opt. Photon.* **3**, 78 (2019).
- [23] Z. Huang, Q. Liu, M. R. Pointer, W. Chen, Y. Liu, Y. Wang, *J. Opt. Soc. Am. A* **37**, A170 (2020).
- [24] S.-M. Yang, P.-H. Wang, C.-H. Chao, C.-W. Chu, Y.-T. Yeh, Y.-S. Chen, F.-P. Chang, Y.-H. Fang, C.-C. Lin, C.-I. Wu, *Opt. Express* **27**, A1308 (2019).
- [25] P. Kaur, Kriti, Rahul, S. Kaur, A. Kandasami, D. P. Singh, *Opt. Lett.* **45**, 3349 (2020).
- [26] X. Y. Huang, S. Y. Wang, B. Li, Q. Sun, H. Guo, *Opt. Lett.* **43**, 1307 (2018).

- [27] L. Vijayalakshmi, K. N. Kumar, P. Hwang, *Opt. Lett.* **44**, 5029 (2019).
- [28] D. T. Tuyet, V. T. H. Quan, B. Bondzior, P. Jacek Dereń, R. T. Velpula, H. P. T. Nguyen, L. A. Tuyen, N. Q. Hung, H. -D. Nguyen, *Opt. Express* **28**, 26189 (2020).
- [29] B. C. Li, D. W. Zhang, Y. S. Huang, Z. J. Ni, S. L. Zhuang, *Chin. Opt. Lett.* **8**, 221 (2010).

---

\*Corresponding author: nguyendoanquocanh@tdtu.edu.vn